

Herzler, Jürgen and Naumann, Clemens,

'Shock Tube Study of the Influence of NO_x on the Ignition Delay Times of Natural Gas at High Pressure',

Combustion Science and Technology, 184: 10, 1635–1650 (2012)

The original publication is available at

<http://dx.doi.org/10.1080/00102202.2012.690617>

Shock Tube Study of the Influence of NO_x on the Ignition Delay Times of Natural Gas at High Pressure

J. Herzler, C. Naumann

Institut für Verbrennungstechnik
Deutsches Zentrum für Luft- und Raumfahrt (DLR)
D-70569 Stuttgart
Germany

Abstract

The ignition delay times of diluted reference gas / O₂ / NO₂ / Ar mixtures ($\Phi = 0.25, 0.5$ and 1.0 , dilution 1:2 and 1:5, [NO₂] = 20 - 250 ppm) were determined in a high-pressure shock tube. The temperature range was $1000 \text{ K} \leq T \leq 1700 \text{ K}$ at pressures of about 16 bar.

The addition of NO₂ leads to a significant reduction of the ignition delay times. This reduction increases with decreasing equivalence ratio. The effect of NO₂ is well predicted by the NO_x chemistry of different published reaction mechanisms. The differences in the predictions of the ignition delay times using a common hydrocarbon reaction mechanism and NO_x subsystems of four published reaction mechanisms are negligible.

Running head: NO_x Influence on the Ignition Delay of Natural Gas

1 Introduction

The influence of NO_x on the combustion characteristics of natural gas is important for the modeling of gas turbines and HCCI engines (Dagaut and Nicolle 2005) with exhaust gas recirculation, and of gas turbines with reheat combustion (Güthe et al. 2009). Exhaust gas recirculation and reheat combustion are used to reduce the combustion temperatures and thus the NO_x production. Purified biogas (methane) or natural gas can be used as fuel in HCCI engines (Dagaut and Nicolle 2005).

Even small amounts of nitrogen oxides lead to significantly shorter ignition delay times (Faravelli et al. 2003, Glarborg 2007) because NO and NO_2 are recycled in the hydrogen and hydrocarbon oxidation environment (Rasmussen et al. 2008). This was found for a variety of systems like H_2 , CO , CH_2O , C_1 , C_2 and higher hydrocarbons, see Rasmussen et al. 2008. This reduction of the ignition delay times is important for the design of HCCI engines because their working principle is the homogeneous ignition by compression. Therefore high pressure data of the influence of NO_x on the oxidation of hydrocarbons are necessary for the design of HCCI engines and also for gas turbines. Only few studies were performed at high pressures, mainly by the group of Dagaut in a jet-stirred reactor (e.g. Dagaut and Nicolle 2005, Dagaut and Dayma 2006), by Rasmussen et al. 2008 in a laminar flow reactor and by Sivaramakrishnan et al. 2007 in a single-pulse shock tube.

There are no ignition delay time studies of natural gas in the presence of NO_x at high pressures despite the importance of these data for modern combustion concepts. Therefore we performed studies at conditions relevant for gas turbine and methane / natural gas HCCI combustion.

Exhaust gas contains CO_2 and H_2O in addition to NO_x . We studied the influence of H_2O at similar conditions to this work and found no significant influence on the ignition delay time with H_2O concentrations of 30 and 50 vol% (Ax et al. 2008). The promoting chemical effect of H_2O on ignition (Reinke et al. 2005) is balanced by its higher heat capacity. There

are only a few other experimental studies of the influence of H₂O or exhaust gas on the ignition delay of hydrocarbons. He et al. 2005 found a slight decrease of the ignition delay times of iso-octane in a rapid compression machine caused by water addition whereas Gauthier et al. 2004 found for the addition of exhaust gas (CO₂ / H₂O / N₂ / O₂) in their shock tube study an increase of the ignition delay times at an equivalence ratio of $\Phi = 1.0$ and no effect at $\Phi = 0.5$ for gasoline and a gasoline surrogate. Reinke et al. 2005 found in their methane ignition experiments over Pt a net increase of the ignition delay times by the addition of 57.1 vol% water. The higher heat capacity of water compared to nitrogen overcompensates the chemical promotion effect which is well predicted by the mechanism of Warnatz et al. 1996. Gurentsov et al. 2002 found a slight increase (20 – 30%) of the ignition delay times of methane with Ar as inert gas caused by a water addition of 9.1 vol%. The same water addition led to a factor of 2 or 3 lower ignition delay times with N₂ as inert gas. Le Cong and Dagaut 2009 observed an inhibiting effect of 10 mol% water on the oxidation of methane in their jet-stirred reactor study.

We studied also the influence of CO₂ on the ignition delay times of natural gas at similar conditions to this work (Herbst et al. 2009). Concentrations of 30 vol% CO₂ lead to an increase of the ignition delay time of up to 30%. At lower temperatures (1100 – 1200 K) this increase is caused mainly by the higher heat capacity of CO₂ compared to Ar. At higher temperatures reactions with CO₂ gain increasing importance for the delayed ignition observed. Sensitivity analyses showed that mainly the reactions



are responsible for the longer ignition delay times. The effect of CO₂ is very well predicted by literature mechanisms, e.g. the RD (RAMEC – DLR) mechanism (Herzler and Naumann 2009). Further studies on of the oxidation of fuels in the presence of CO₂ were performed in a flow reactor by Glarborg and Bentzen 2008 and in a jet-stirred reactor by Le Cong and Dagaut 2008.

2 Experimental Setup

The experiments were carried out in a high pressure shock tube with an internal diameter of 98.2 mm. It is divided by aluminium diaphragms into a driver section of 5.18 m and a driven section of 11.12 m in length. The driven section can be pumped down to pressures below 10^{-6} mbar by a turbomolecular pump. Gas mixtures were prepared manometrically in a stainless steel storage cylinder, which is evacuated using a separate turbomolecular pump to pressures below 10^{-6} mbar. The shock speed was measured over three 20 cm intervals using four piezoelectric pressure gauges. The temperature and pressure behind the reflected shock wave were computed from the measured incident shock speed and the speed attenuation using a one-dimensional shock model. The estimated uncertainty in reflected shock temperature is less than ± 15 K in the temperature range of our measurements.

The ignition was observed by measuring pressure profiles with piezoelectric gauges (PCB[®] 113A24 and Kistler[®] 603B) located at a distance of 1 cm to the end flange. The PCB[®] gauge was shielded by 1 mm polyimide to reduce heat transfer. Also, the CH* emission at 431 nm at the same position was selected by a narrow band pass filters (FWHM = 5 nm) and measured with a photomultiplier. All ignition delay time values shown in this paper were determined by measuring the time difference between the initiation of the system by the reflected shock wave and the occurrence of the CH* maximum because this allows a good comparability to simulations. The experimental setup allows measurements of ignition delay times for observation times up to 6.5 ms depending on the temperature.

3 Results and Discussion

The ignition delay times of reference gas (92% methane, 8% ethane) – a natural gas model fuel – mixtures with NO₂ were determined at three different equivalence ratios. The fuel / oxygen / NO₂ / argon mixtures ($\Phi = 0.25, 0.5$ and 1.0 , [O₂] / [Ar] = 21 vol% / 79 vol%) were diluted with argon (50% mixture / 50% Ar, defined as dilution 1:2, 20% mixture / 80%

Ar, defined as dilution 1:5). NO₂ concentrations of 20 – 251 ppm were used. NO₂ was used instead of NO because NO is rapidly oxidized by O₂ at room temperature (Glasson and Tuesday 1963). The temperature range was $1000\text{ K} \leq T \leq 1700\text{ K}$ at pressures of about 16 bar. A table of all mixtures used is given in the supplemental material. A typical pressure and CH*-emission profile is shown in Fig. 1. The pressure signal of a reference gas / O₂ / NO₂ / Ar mixture ($\Phi = 1.0$, dilution 1:5, 103 ppm NO₂) at $T = 1264\text{ K}$ and $p = 15.91\text{ bar}$ (black line) shows a two-step increase due to the incident and reflected shock wave (time zero), then a very slight pressure increase due to gas-dynamic effects for about 1500 μs , followed by a stronger increase due to heat release of the reacting system and a steep rise at 2680 μs due to ignition. The CH* emission (gray line) remains at zero level for 2680 μs , followed by a steep rise indicating ignition.

The individual ignition delay times evaluated from the CH*-emission signals are summarized in Figs. 2-5. A list of all experimental results is given in the supplemental material. Even small amounts of NO₂ lead to significantly lower ignition delay times (up to a factor of 3). The influence of NO₂ on ignition delay times is increasing with decreasing equivalence ratio. The measured data were compared to MPFR-CHEMKIN II (Kee et al. 1989) predictions using the reaction mechanisms of Rasmussen et al. 2008, Sivaramakrishnan et al. 2007, Hori et al. 1998 and Faravelli et al. 2003. Reactions leading to chemiluminescence like $\text{C}_2\text{H} + \text{O} \rightleftharpoons \text{CH}^* + \text{CO}$, $\text{CH} + \text{O}_2 \rightleftharpoons \text{CO} + \text{OH}^*$, $\text{H} + \text{O} + \text{M} \rightleftharpoons \text{OH}^* + \text{M}$ and thermal and spectroscopic deexcitation reactions of CH* and OH* (Smith et al. 2002) were added to all mechanisms for comparison with the experimentally detected chemiluminescence maxima.

MPFR (Multiple Plug Flow Reactor) - CHEMKIN II (Kee et al. 1989) is a programme developed at DLR Stuttgart to take into account gas-dynamic effects causing pressure and temperature variations decoupled from the effects of heat release combined with pressure relaxation effects along the shock propagation direction due to the shock tube's 'open end' configuration. Thus, the simulation assumes for a time period of typically 25 μs or shorter

depending on the heat release ($\Delta T \leq 0.5\%$) a PFR with constant pressure conditions and takes into account the propagation of the pressure increase by heat release within a PFR-time step along the shock propagation direction. The correction of the gas-dynamic effects is based on the pressure profiles measured of mixtures with similar acoustic properties but without heat release by chemical reactions. The temperature profiles are then calculated by applying adiabatic and isentropic conditions. These temperature profiles were used instead of constant initial temperatures T_5 for the simulation of experimental profiles with different chemical mechanisms.

Simulations with literature mechanisms of Rasmussen et al. 2008, Sivaramakrishnan et al. 2007, Hori et al. 1998 and Faravelli et al. 2003. show a good prediction of the shortening of the ignition delay times by NO_2 , see Figs. 2-6. A comparison of the different NO_x -submodels is quite difficult because the predictions of the mechanisms for the natural gas model fuel without NO_x addition differ significantly, see Figs. 2-6. Therefore we combined the NO_x -submodels with our RD mechanism (Herzler and Naumann 2009), which is based on the RAMEC (RAM accelerator MECHANISM) mechanism of Petersen et al. 1999 with additions made at DLR Stuttgart concerning the C_2H_5 , the formaldehyde, the acetaldehyde and the C_2H_6 system. The RD mechanism, which predicts the ignition delay times of the natural gas model fuel at all equivalence ratios and temperatures used very well, is available on request. The RD mechanism is validated for natural gas and temperatures $T > 950$ K. Figures 7-11 show that the shortening of the ignition delay times by NO_2 is very well predicted by all NO_x -submodels (Rasmussen et al. 2008, Sivaramakrishnan et al. 2007, Hori et al. 1998 and Faravelli et al. 2003). The difference between the NO_x submodels is negligible.

Figure 12 shows the differences of simulations with a constant initial temperature and with a temperature profile derived from the measured pressure profiles of non-reacting mixtures presented in Fig. 13. The pressure increase $dp/(p dt)$ averages 2.0% / ms. By applying adiabatic isentropic conditions the pressure increase of the non-reacting mixtures can be

converted to a temperature increase of about 20 K at 2.5 ms and 40 K at 5 ms. Up to ignition delay times < 2 ms the influence of the temperature increase caused by gas-dynamic effects is negligible. For longer ignition delay times the effect of this temperature increase lead to a significant reduction of the ignition delay times compared to the simulations with constant initial temperature and to a good agreement with the simulations for the lowest temperatures. We performed sensitivity analyses of the ignition delay times at 1100 and 1300 K by multiplying the individual rate coefficients with factors of 0, 0.5 and 2. The most important reactions describing the influence of NO_x at our conditions characterized by high pressure and low NO_x concentrations are shown in Figures 14-15. The main reactions of NO_x are



With increasing temperature



gains importance.

NO and NO_2 lead to shorter ignition delay times by reactions R3 and R4. They are closely related by the cycle shown in Fig. 16. NO_2 is fast converted to NO by reaction R3. The very good prediction of the influence of NO_2 on the ignition delay of natural gas is only possible if the reactions of not only NO_2 but also NO are well-described by the mechanisms. Therefore they are very well suited for simulating natural gas / NO mixtures which are of interest because NO is the main NO_x species which is formed during combustion. The calculated influence of NO on the ignition delay times of our natural gas model fuel is about half as strong as the one of NO_2 , see Figures 17-19. The different NO_x -submodels of Sivaramakrishnan et al. 2007 and Hori et al. 1998 show again very similar results whereas the

models of Faravelli et al. 2003 and of Rasmussen et al. 2008 predicts slightly longer ignition delay times especially at lower temperatures, see Fig. 20.

4 Conclusions

The current work presents data at gas turbine relevant pressure and temperature conditions for ignition delay times of natural gas in the presence of NO_x , which are important for exhaust gas recirculation and for gas turbines with reheat combustion. Even small amounts of NO_x lead to significantly shorter ignition delay times (up to a factor of 3), especially at lean conditions. It was shown that all tested NO_x literature mechanisms (Rasmussen et al. 2008, Sivaramakrishnan et al. 2007, Hori et al. 1998 and Faravelli et al. 2003) are very well-suited for predicting the influence of NO_x on the ignition delay times. These mechanisms can only predict the trends with NO_x addition but not the absolute values of the ignition delay times because their hydrocarbon chemistry is not well-suited for simulating the ignition of natural gas at gas-turbine typical conditions. By combining the hydrocarbon chemistry of the RD mechanism (Herzler and Naumann 2009) with the NO_x chemistry of the other mechanisms a very good agreement of simulations and experiments was found. The differences of the predictions using the different NO_x chemistry models are negligible.

5 Acknowledgement

The authors thank the Ministerium für Wissenschaft, Forschung und Kunst of Baden-Württemberg for its financial support of the work within the project “Kraftwerke des 21. Jahrhunderts” (KW21 GV2-AP1). Furthermore, the authors thank ALSTOM Switzerland for their interest and support.

6 References

Ax, H., Koch, A., Naumann, C., Sadanandan, R., Dreyer, A. and Herzler, J., GV 2: Zünd- und Löschverhalten von Erdgasen in Gasturbinenbrennkammern: Erhöhung der Zuverlässigkeit, in: Abschlussbericht Phase I Forschungsinitiative „Kraftwerke des 21. Jahrhunderts (KW21)“, 2008

Dagaut, P. and Dayma, G. (2006) Mutual sensitization of the oxidation of nitric oxide and a natural gas blend in a JSR at elevated pressure: Experimental and detailed kinetic modeling study, *J. Phys. Chem. A*, **110**, 6608.

Dagaut, P. and Nicolle, A. (2005) Experimental study and detailed kinetic modeling of the effect of exhaust gas on fuel combustion: mutual sensitization of the oxidation of nitric oxide and methane over extended temperature and pressure ranges, *Combust. Flame*, **140**, 161.

Faravelli, T., Frassoldati, A. and Ranzi, E. (2003) Kinetic modeling of the interactions between NO and hydrocarbons in the oxidation of hydrocarbons at low temperatures, *Combust. Flame*, **132**, 188.

Kinetic Mechanism version 1101 (January, 2011), C1-C3 mechanism, Kinetic scheme with NOx, <http://creckmodeling.chem.polimi.it/kinetic.html>

Gauthier, B.M., Davidson, D.F. and Hanson, R.K. (2004) Shock tube determination of ignition delay times in full-blend and surrogate fuel mixtures, *Comb. Flame*, **139**, 300.

Glarborg, P. (2007) Hidden interactions - Trace species governing combustion and emissions, *Proc. Combust. Inst.*, **31**, 77.

Glarborg, P., and Bentzen, L.L.B (2008) Chemical Effects of a High CO₂ Concentration in Oxy-Fuel Combustion of Methane, *Energy & Fuels*, **22**, 291.

Glasson, W.A. and Tuesday, C.S. (1963) The atmospheric thermal oxidation of nitric oxide, *J. Am. Chem. Soc.*, **85**, 2901.

Gurentsov, E.V., Divakov, O.G. and Eremin, A.V. (2002), Ignition of Multicomponent Hydrocarbon/Air Mixtures behind Shock Waves, *High Temp.*, **40**, 379.

Güthe, F., Hellat, J. and Flohr, P. (2009) The Reheat Concept: The Proven Pathway to Ultralow Emissions and High Efficiency and Flexibility, *J. Eng. Gas Turbines Power*, **131**, 021503 1.

He, X., Donovan, M.T., Zigler, B.T., Palmer, T.R., Walton, S.M., Wooldrigde, M.S. and Atreay, A. (2005) An experimental and modeling study of iso-octane ignition delay times under homogeneous charge compression ignition conditions, *Comb. Flame*, **142**, 266.

Herbst, J., Herzler, J., Kick, T. and Naumann, C. (2009), Untersuchung der Verbrennung von Erdgasreferenzbrennstoff bei Oxyfuel-Bedingungen, *VDI-Berichte*, **2056**, 211.

Herzler, J. and Naumann, C. (2009) Shock-tube study of the ignition of methane/ethane/hydrogen mixtures with hydrogen contents from 0% to 100% at different pressures, *Proc. Combust. Inst.*, **32**, 213.

Hori, M., Matsunaga, N., Marinov, N.M., Pitz, W.J. and Westbrook, C.K. (1998) An experimental and kinetic calculation of the promotion effect of hydrocarbons on the NO-NO₂ conversion in a flow reactor, *Proc. Combust. Inst.*, **27**, 389.

Kee, R.J., Rupley, F.M. and Miller, J.A. (1989) Chemkin-II: A Fortran chemical kinetics package for the analysis of gas-phase chemical kinetics, Report No. SAND89-8009, Sandia National Laboratories.

Le Cong, T. and Dagaut, P. (2008) Experimental and detailed kinetic modeling of the oxidation of methane and methane/syngas mixtures and effect of carbon dioxide addition, *Combust. Sci. Technol.*, **180**, 2046.

Le Cong, T. and Dagaut, P. (2009) Experimental and Detailed Modeling Study of the Effect of Water Vapor on the Kinetics of Combustion of Hydrogen and Natural Gas, Impact on NO_x, *Energy&Fuels*, **23**, 725.

Petersen, E.L., Davidson D.F. and Hanson R.K. (1999) Kinetics modeling of shock-induced ignition in low-dilution CH₄/O₂ mixtures at high pressures and intermediate temperatures, *Combust. Flame*, **117**, 272.

Rasmussen, C.L., Rasmussen, A.E. and Glarborg, P. (2008) Sensitizing effects of NO_x on CH₄ oxidation at high pressure, *Combust. Flame*, **154**, 529.

Reinke, M., Mantzaras, J., Schaeren, R., Bombach, R., Inauen, A. and Schenker, S. (2005) Homogeneous ignition of CH₄/air and H₂O and CO₂-diluted CH₄/O₂ mixtures over Pt; an experimental and numerical investigation at pressures up to 16 bar, *Proc. Combust. Inst.*, **30**, 2519.

Sivaramakrishnan, R., Brezinsky, K., Dayma, G. and Dagaut, P. (2007) High pressure effects on mutual sensitization of the oxidation of NO and CH₄-C₂H₆ blends. *Phys. Chem. Chem. Phys.*, **9**, 4230.

Smith, G.P., Luque, J., Chung, P., Jeffries, J.B. and Crosley, D.R. (2002) Low pressure flame determinations of rate constants for OH(A) and CH(A) chemiluminescence, *Combust. Flame*, **131**, 59.

Warnatz, J., Dibble, R.W. and Maas, U., *Combustion, Physical and Chemical Fundamentals, Modeling and Simulation*. Springer-Verlag, New York, 1996, p.69.

Figure Captions

Fig. 1: Typical pressure (black line) and CH*-emission (gray line) profiles indicating ignition delay in a lean, diluted ($\Phi = 1.0$, dilution 1:5, 103 ppm NO₂) reference gas / Ar / NO₂ / O₂ mixture. Reaction conditions: $T_5 = 1264$ K, $p_5 = 15.91$ bar.

Fig. 2: Measured and calculated ignition delay times for mixtures of reference gas / O₂ / (NO₂) / Ar ($\Phi = 0.25$, dilution 1:2) at pressures of about 16 bar. Experiments: 0 ppm NO₂: squares, 50 ppm NO₂: triangles, 251 ppm NO₂: circles. MPFR-CHEMKIN II (Kee et al. 1989) simulations: Rasmussen et al. 2008 mechanism: black lines, Sivaranakrishnan et al. 2007 mechanism: gray lines. 0 ppm NO₂: full lines, 50 ppm NO₂: dashed lines, 251 ppm NO₂: dashed-dotted lines.

Fig. 3: Measured and calculated ignition delay times for mixtures of reference gas / O₂ / (NO₂) / Ar ($\Phi = 0.25$, dilution 1:5) at pressures of about 16 bar. Experiments: 0 ppm NO₂: squares, 20 ppm NO₂: triangles, 101 ppm NO₂: circles. MPFR-CHEMKIN II (Kee et al. 1989) simulations: Rasmussen et al. 2008 mechanism: black lines, Sivaranakrishnan et al. 2007 mechanism: gray lines. 0 ppm NO₂: full lines, 20 ppm NO₂: dashed lines, 101 ppm NO₂: dashed-dotted lines.

Fig. 4: Measured and calculated ignition delay times for mixtures of reference gas / O₂ / (NO₂) / Ar ($\Phi = 0.5$, dilution 1:5) at pressures of about 16 bar. Experiments: 0 ppm NO₂: squares, 20 ppm NO₂: triangles, 100 ppm NO₂: circles. MPFR-CHEMKIN II (Kee et al. 1989) simulations: Rasmussen et al. 2008 mechanism: black lines, Sivaranakrishnan et al. 2007 mechanism: gray lines. 0 ppm NO₂: full lines, 20 ppm NO₂: dashed lines, 100 ppm NO₂: dashed-dotted lines.

Fig. 5: Measured and calculated ignition delay times for mixtures of reference gas / O₂ / (NO₂) / Ar ($\Phi = 1.0$, dilution 1:5) at pressures of about 16 bar. Experiments: 0 ppm NO₂: squares, 100 ppm NO₂: circles. MPFR-CHEMKIN II (Kee et al. 1989)

simulations: Rasmussen et al. 2008 mechanism: black lines, Sivaranakrishnan et al. 2007 mechanism: gray lines. 0 ppm NO₂: full lines, 100 ppm NO₂: dashed-dotted lines.

Fig. 6: Measured and calculated ignition delay times for mixtures of reference gas / O₂ / (NO₂) / Ar ($\Phi = 0.25$, dilution 1:5) at pressures of about 16 bar. Experiments: 0 ppm NO₂: squares, 20 ppm NO₂: triangles, 101 ppm NO₂: circles. MPFR-CHEMKIN II (Kee et al. 1989) simulations: Hori et al. 1998 mechanism: black lines, Faravelli et al. 2003 mechanism: gray lines. 0 ppm NO₂: full lines, 20 ppm NO₂: dashed lines, 101 ppm NO₂: dashed-dotted lines.

Fig. 7: Measured and calculated ignition delay times for mixtures of reference gas / O₂ / (NO₂) / Ar ($\Phi = 0.25$, dilution 1:2) at pressures of about 16 bar. Experiments: 0 ppm NO₂: squares, 50 ppm NO₂: triangles, 251 ppm NO₂: circles. MPFR-CHEMKIN II (Kee et al. 1989) simulations: RD-mechanism (Herzler and Naumann 2009) with NO_x chemistry of Rasmussen et al. 2008: black lines, RD-mechanism (Herzler and Naumann 2009) with NO_x chemistry of Sivaranakrishnan et al. 2007: gray lines. 0 ppm NO₂: full lines, 50 ppm NO₂: dashed lines, 251 ppm NO₂: dashed-dotted lines.

Fig. 8: Measured and calculated ignition delay times for mixtures of reference gas / O₂ / (NO₂) / Ar ($\Phi = 0.25$, dilution 1:5) at pressures of about 16 bar. Experiments: 0 ppm NO₂: squares, 20 ppm NO₂: triangles, 101 ppm NO₂: circles. MPFR-CHEMKIN II (Kee et al. 1989) simulations: RD-mechanism (Herzler and Naumann 2009) with NO_x chemistry of Rasmussen et al. 2008: black lines, RD-mechanism (Herzler and Naumann 2009) with NO_x chemistry of Sivaranakrishnan et al. 2007: gray lines. 0 ppm NO₂: full lines, 20 ppm NO₂: dashed lines, 101 ppm NO₂: dashed-dotted lines.

Fig. 9: Measured and calculated ignition delay times for mixtures of reference gas / O₂ / (NO₂) / Ar ($\Phi = 0.5$, dilution 1:5) at pressures of about 16 bar. Experiments: 0 ppm NO₂: squares, 20 ppm NO₂: triangles, 100 ppm NO₂: circles. MPFR-CHEMKIN II (Kee et al. 1989) simulations: RD-mechanism (Herzler and Naumann 2009) with NO_x chemistry of Rasmussen et al. 2008: black lines, RD-mechanism (Herzler and

Naumann 2009) with NO_x chemistry of Sivaranakrishnan et al. 2007: gray lines.
0 ppm NO_2 : full lines, 20 ppm NO_2 : dashed lines, 100 ppm NO_2 : dashed-dotted lines.

Fig. 10: Measured and calculated ignition delay times for mixtures of reference gas / O_2 / (NO_2) / Ar ($\Phi = 1.0$, dilution 1:5) at pressures of about 16 bar. Experiments: 0 ppm NO_2 : squares, 100 ppm NO_2 : circles. MPFR-CHEMKIN II (Kee et al. 1989) simulations: RD-mechanism (Herzler and Naumann 2009) with NO_x chemistry of Rasmussen et al. 2008: black lines, RD-mechanism (Herzler and Naumann 2009) with NO_x chemistry of Sivaranakrishnan et al. 2007: gray lines. 0 ppm NO_2 : full lines, 100 ppm NO_2 : dashed-dotted lines.

Fig. 11: Measured and calculated ignition delay times for mixtures of reference gas / O_2 / (NO_2) / Ar ($\Phi = 0.25$, dilution 1:5) at pressures of about 16 bar. Experiments: 0 ppm NO_2 : squares, 20 ppm NO_2 : triangles, 101 ppm NO_2 : circles. MPFR-CHEMKIN II (Kee et al. 1989) simulations: RD-mechanism (Herzler and Naumann 2009) with NO_x chemistry of Hori et al. 1998: black lines, RD-mechanism (Herzler and Naumann 2009) with NO_x chemistry of Faravelli et al. 2003: gray lines. 0 ppm NO_2 : full lines, 20 ppm NO_2 : dashed lines, 101 ppm NO_2 : dashed-dotted lines.

Fig. 12: Measured and calculated ignition delay times for mixtures of reference gas / O_2 / (NO_2) / Ar ($\Phi = 0.5$, dilution 1:5) at pressures of about 16 bar. Experiments: 0 ppm NO_2 : squares, 20 ppm NO_2 : triangles, 100 ppm NO_2 : circles. MPFR-CHEMKIN II (Kee et al. 1989) simulations using the RD-mechanism (Herzler and Naumann 2009) with NO_x chemistry of Rasmussen et al. 2008: black lines: simulations considering the temperature increase due to gas-dynamic effects, gray lines: simulations without temperature increase. 0 ppm NO_2 : full lines, 20 ppm NO_2 : dashed lines, 100 ppm NO_2 : dashed-dotted lines.

Fig. 13: Measured pressure and calculated temperature profile of Ar at an initial pressure $p_5 = 15.84$ bar and an initial temperature $T_5 = 1053$ K. Black line: pressure profile

measured with a Kistler[®] 603B pressure transducer. Gray line: calculated temperature profile assuming adiabatic isentropic conditions.

Fig. 14: Sensitivity analysis of the ignition delay times for a mixture of reference gas / O₂ / NO₂ / Ar ($\Phi = 0.25$, dilution 1:5, [NO₂] = 101 ppm) at a pressure of 16 bar and a temperature of 1100 K using the RD-mechanism (Herzler and Naumann 2009) with NO_x chemistry of Rasmussen et al. 2008. The most sensitive reactions of the NO_x cycle are shown.

Fig. 15: Sensitivity analysis of the ignition delay times for a mixture of reference gas / O₂ / NO₂ / Ar ($\Phi = 0.25$, dilution 1:5, [NO₂] = 101 ppm) at a pressure of 16 bar and a temperature of 1300 K using the RD-mechanism (Herzler and Naumann 2009) with NO_x chemistry of Rasmussen et al. 2008. The most sensitive reactions of the NO_x cycle are shown.

Fig. 16: Most important reactions of NO_x during natural gas oxidation at high pressures, intermediate temperatures and low NO_x concentrations.

Fig. 17: Calculated and (measured) ignition delay times for mixtures of reference gas / O₂ / (NO₂) / (NO) / Ar ($\Phi = 0.25$, dilution 1:2) at pressures of about 16 bar. Experiments: 0 ppm NO₂: squares, 50 ppm NO₂: triangles, 251 ppm NO₂: circles. MPFR-CHEMKIN II (Kee et al. 1989) simulations using the RD-mechanism (Herzler and Naumann 2009) with NO_x chemistry of Sivaranakrishnan et al. 2007: simulations with NO₂: black lines, simulations with NO: gray lines. 0 ppm NO₂ / NO: full lines, 50 ppm NO₂ / NO: dashed lines, 251 ppm NO₂ / NO: dashed-dotted lines.

Fig. 18: Calculated and (measured) ignition delay times for mixtures of reference gas / O₂ / (NO₂) / (NO) / Ar ($\Phi = 0.25$, dilution 1:5) at pressures of about 16 bar. Experiments: 0 ppm NO₂: squares, 20 ppm NO₂: triangles, 101 ppm NO₂: circles. MPFR-CHEMKIN II (Kee et al. 1989) simulations using the RD-mechanism (Herzler and Naumann 2009) with NO_x chemistry of Sivaranakrishnan et al. 2007: simulations with

NO₂: black lines, simulations with NO: gray lines. 0 ppm NO₂ / NO: full lines, 20 ppm NO₂ / NO: dashed lines, 101 ppm NO₂ / NO: dashed-dotted lines.

Fig. 19: Calculated and (measured) ignition delay times for mixtures of reference gas / O₂ / (NO₂) / (NO) / Ar ($\Phi = 0.5$, dilution 1:5) at pressures of about 16 bar. Experiments: 0 ppm NO₂: squares, 20 ppm NO₂: triangles, 100 ppm NO₂: circles. MPFR-CHEMKIN II (Kee et al. 1989) simulations using the RD-mechanism (Herzler and Naumann 2009) with NO_x chemistry of Sivaranakrishnan et al. 2007: simulations with NO₂: black lines, simulations with NO: gray lines. 0 ppm NO₂ / NO: full lines, 20 ppm NO₂ / NO: dashed lines, 100 ppm NO₂ / NO: dashed-dotted lines.

Fig. 20: Calculated ignition delay times for mixtures of reference gas / O₂ / NO / Ar ($\Phi = 0.25$, dilution 1:2, [NO] = 251 ppm) at a pressure of 16 bar. MPFR-CHEMKIN II (Kee et al. 1989) simulations using the RD-mechanism (Herzler and Naumann 2009) with NO_x chemistry of Sivaranakrishnan et al. 2007: full line, Rasmussen et al. 2008: dashed line, Hori et al. 1998: dotted line, Faravelli et al. 2003: dashed-dotted line.

Figures

Figure 1

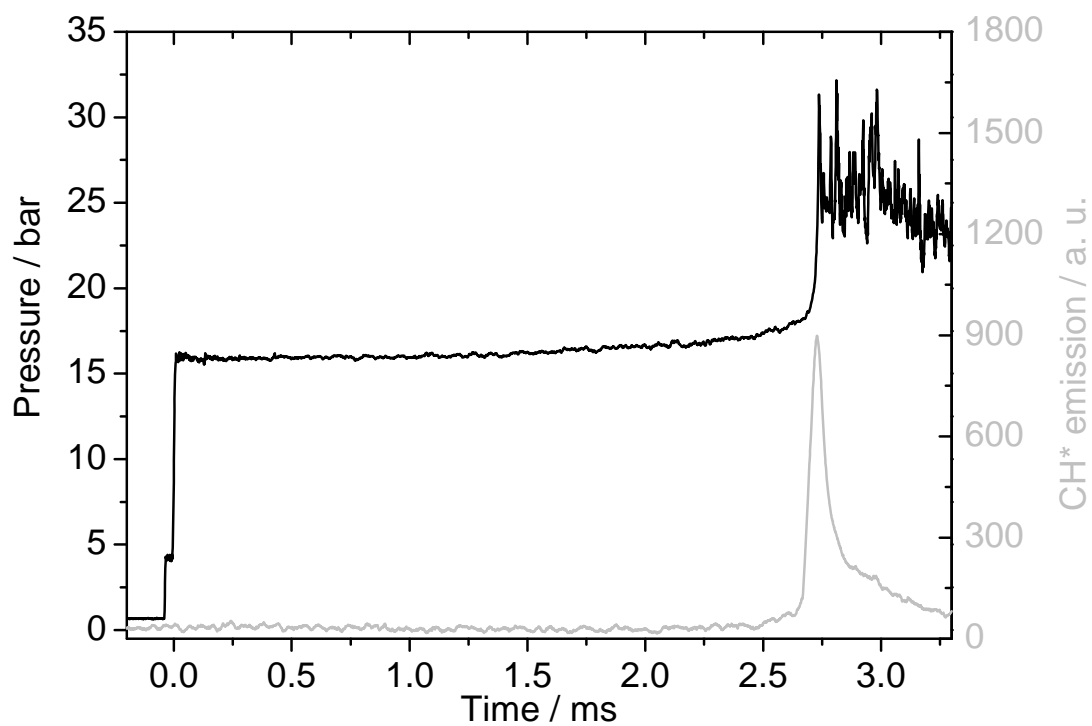


Figure 2

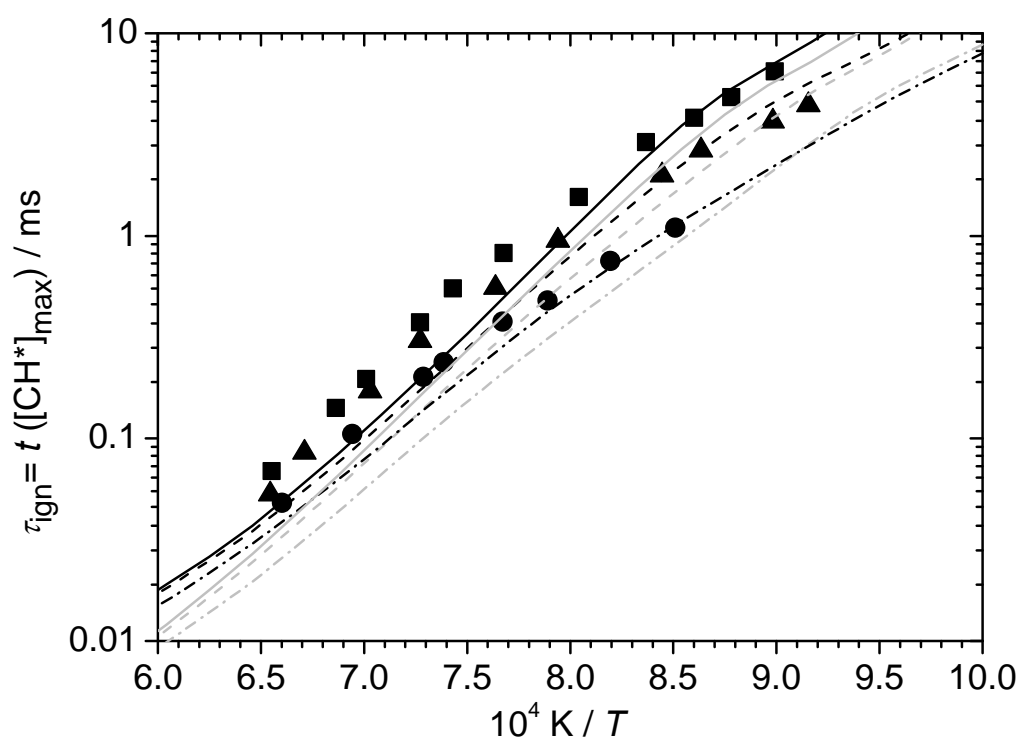


Figure 3

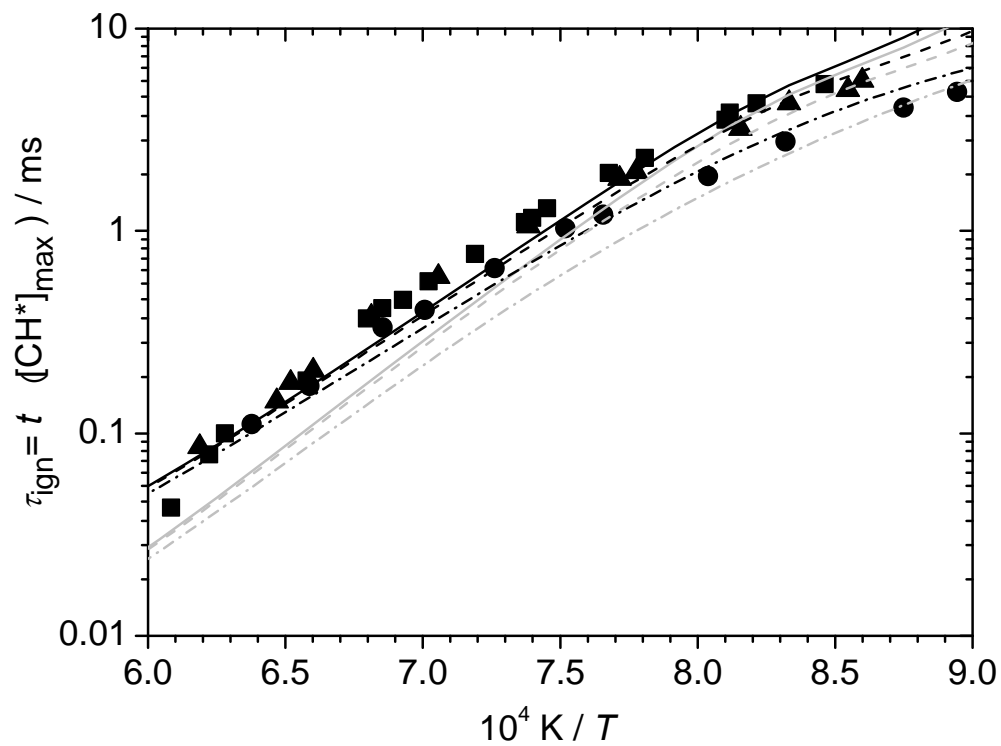


Figure 4

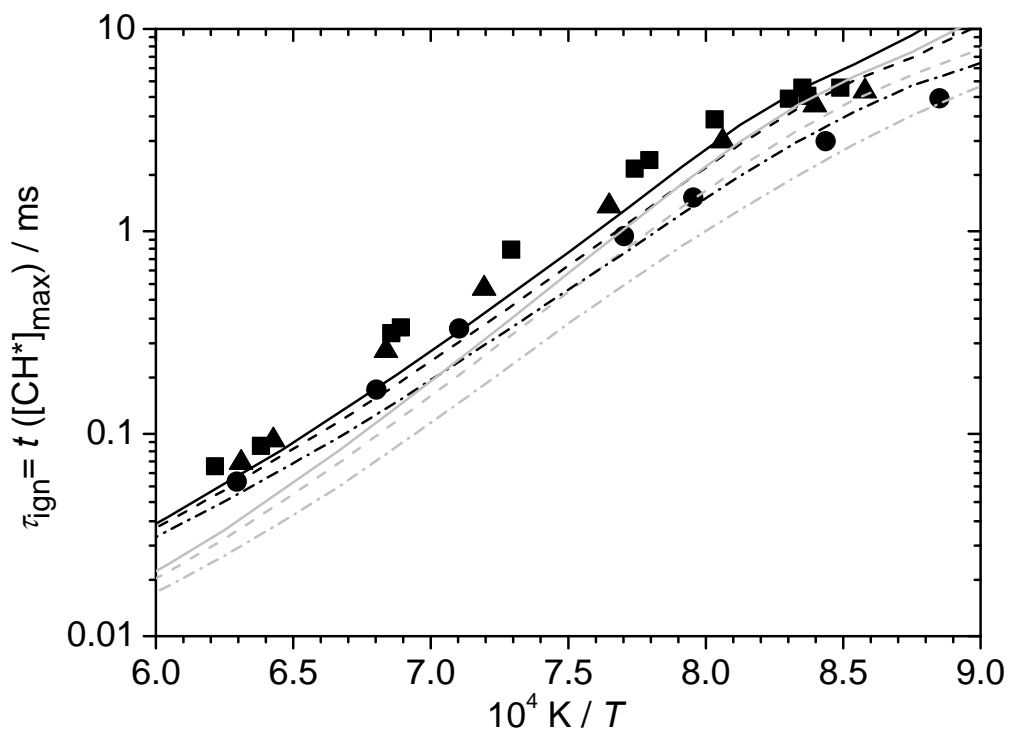


Figure 5

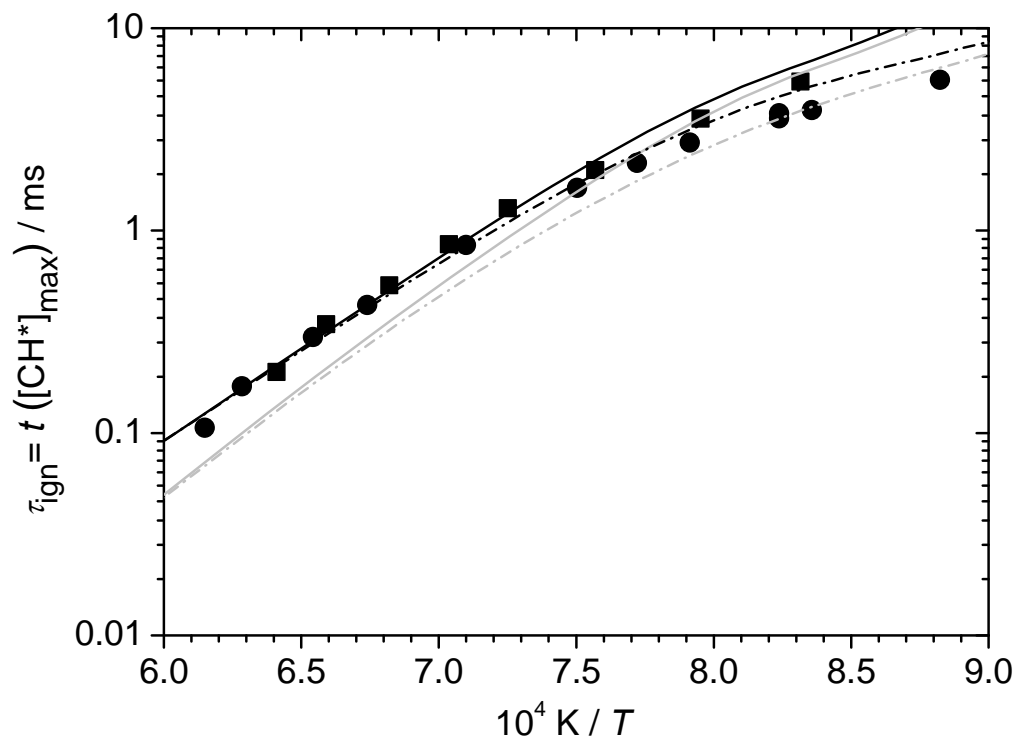


Figure 6

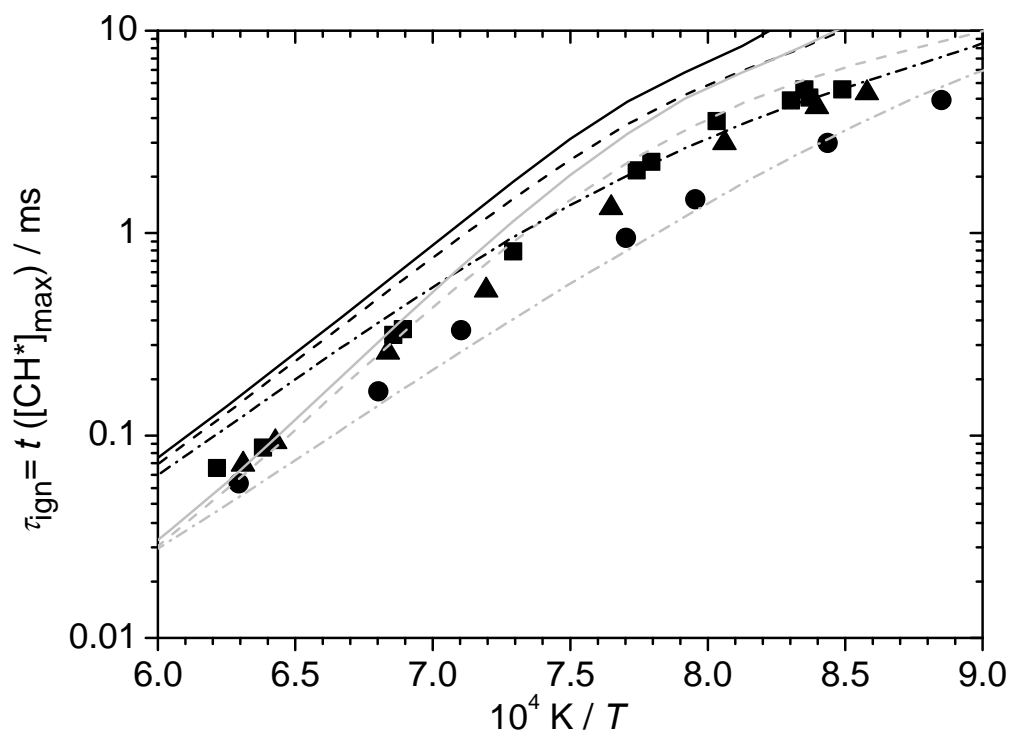


Figure 7

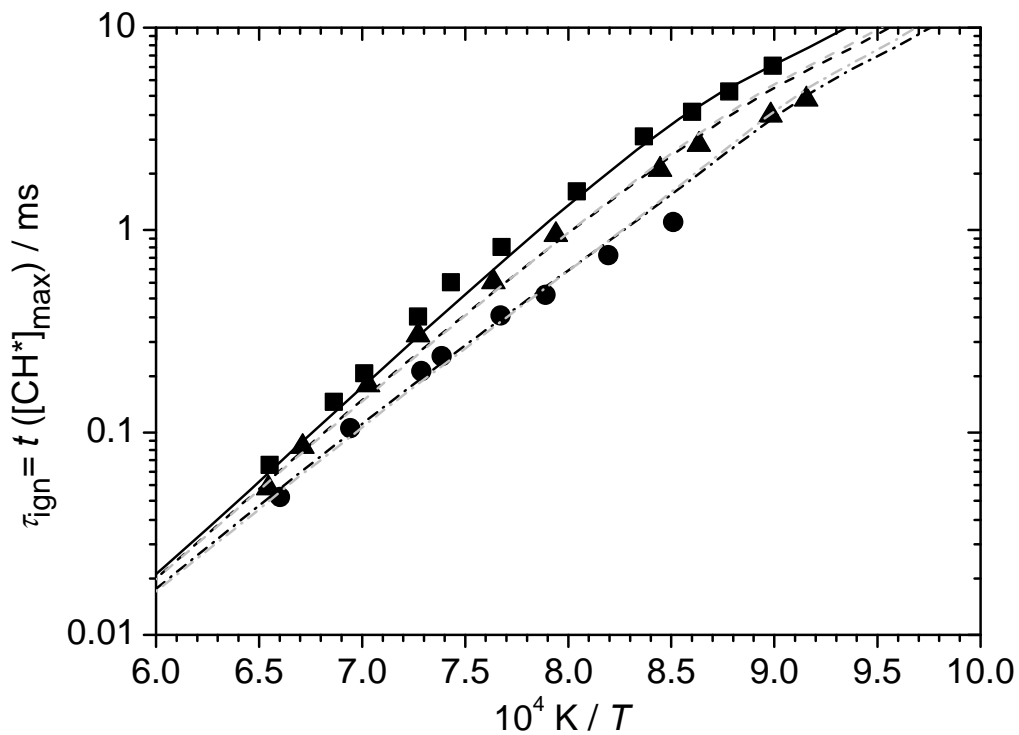


Figure 8

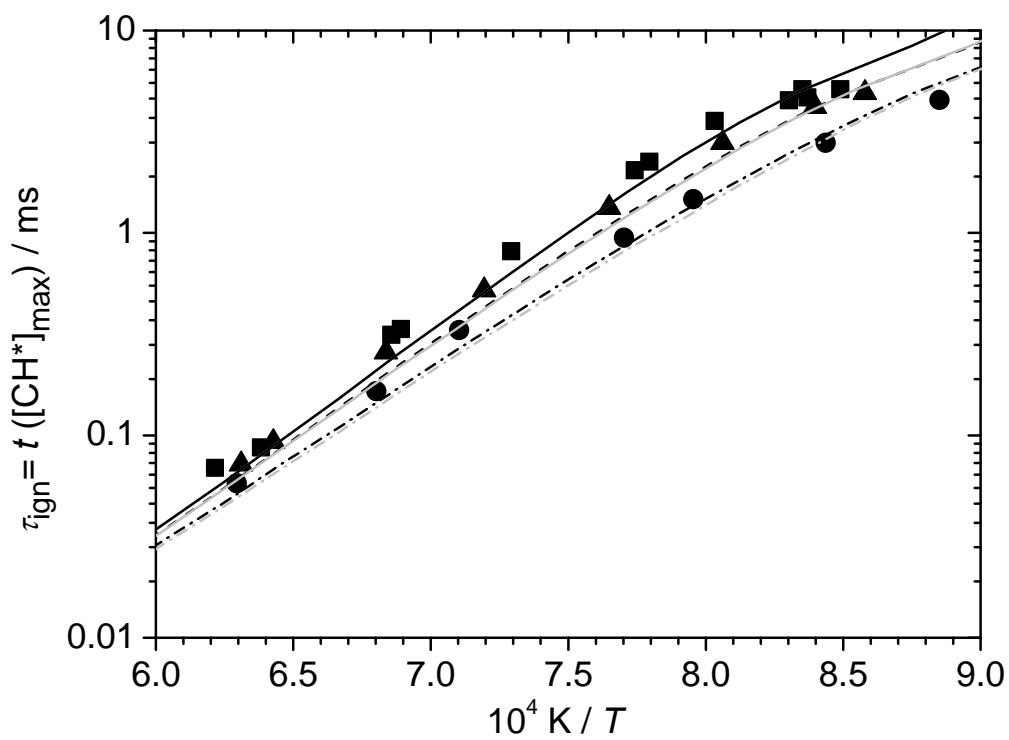


Figure 9

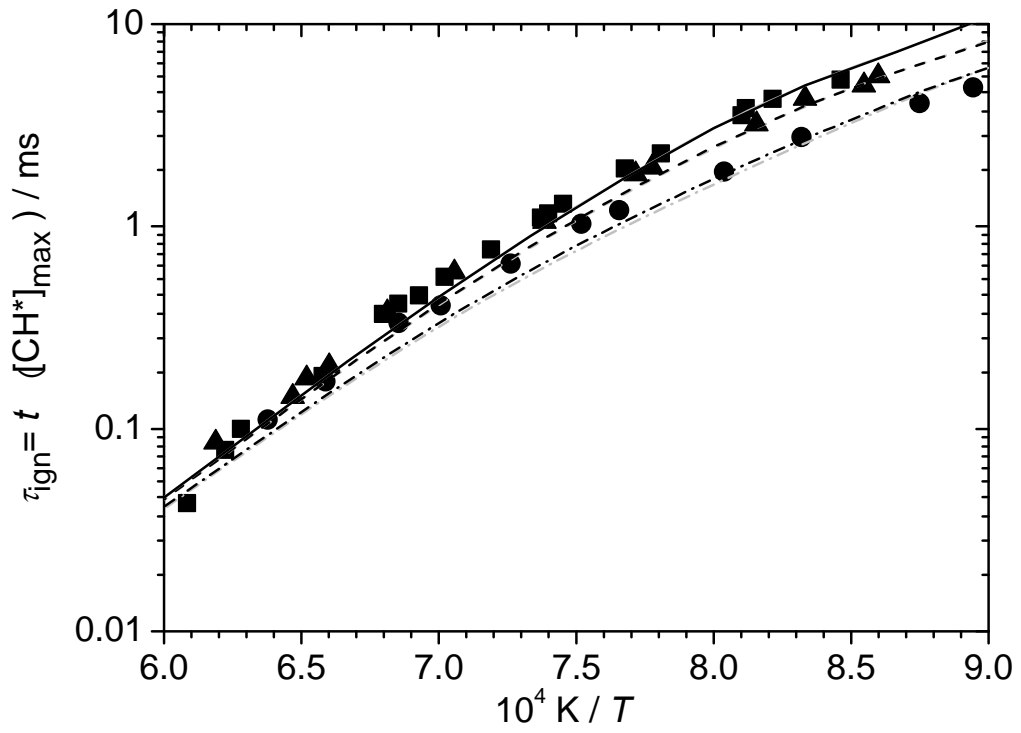


Figure 10

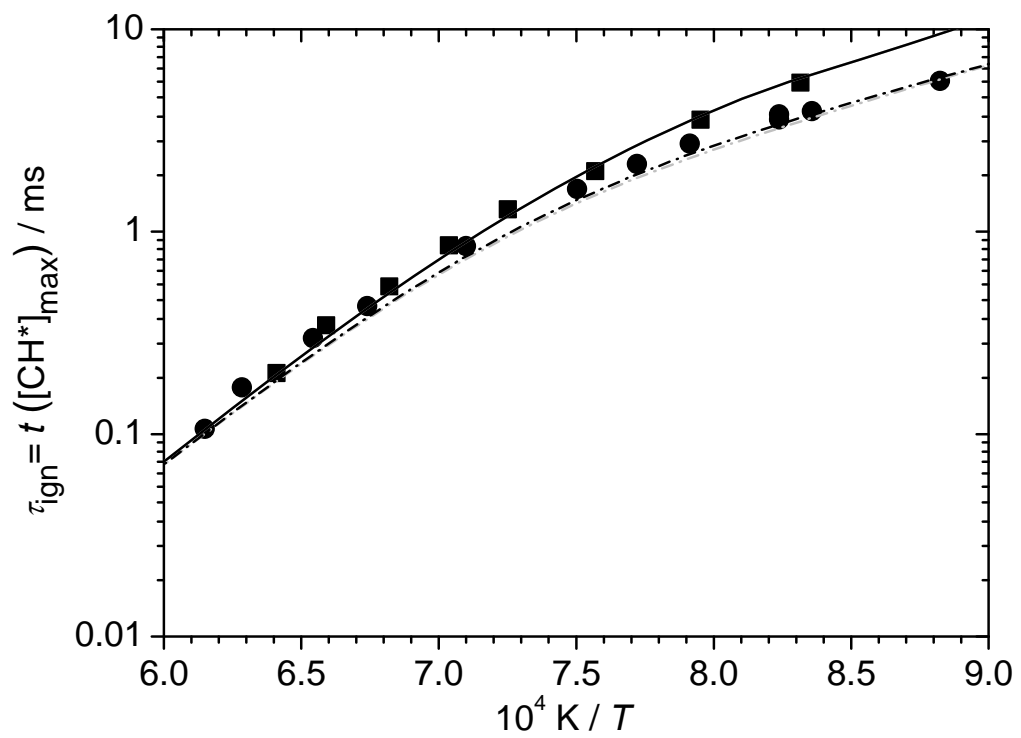


Figure 11

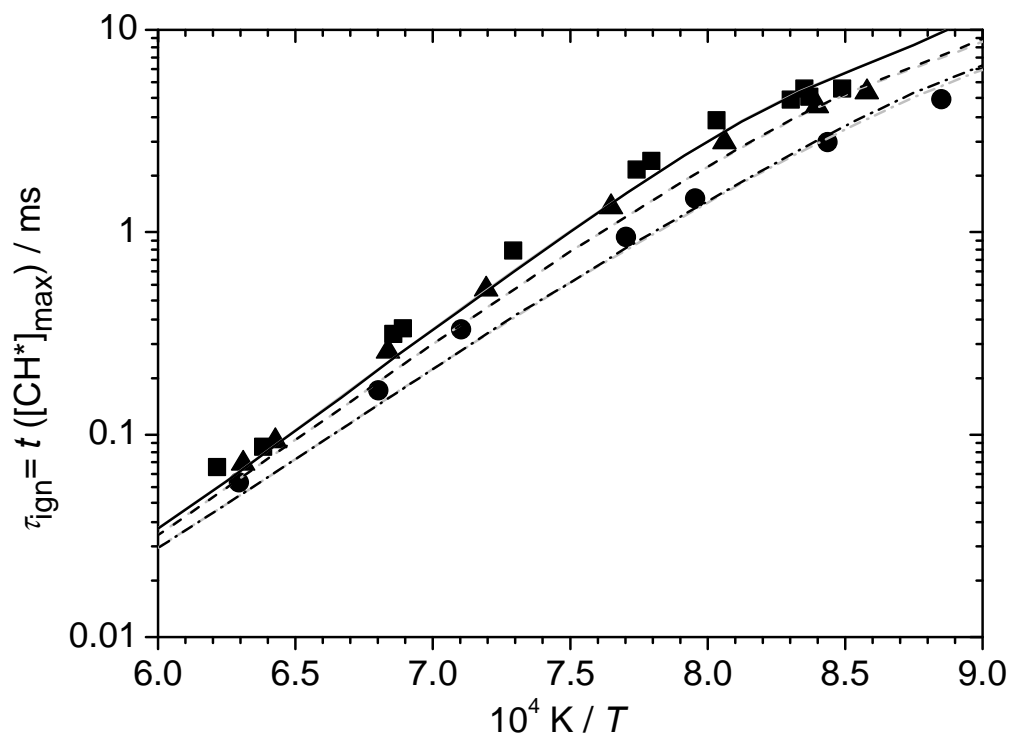


Figure 12

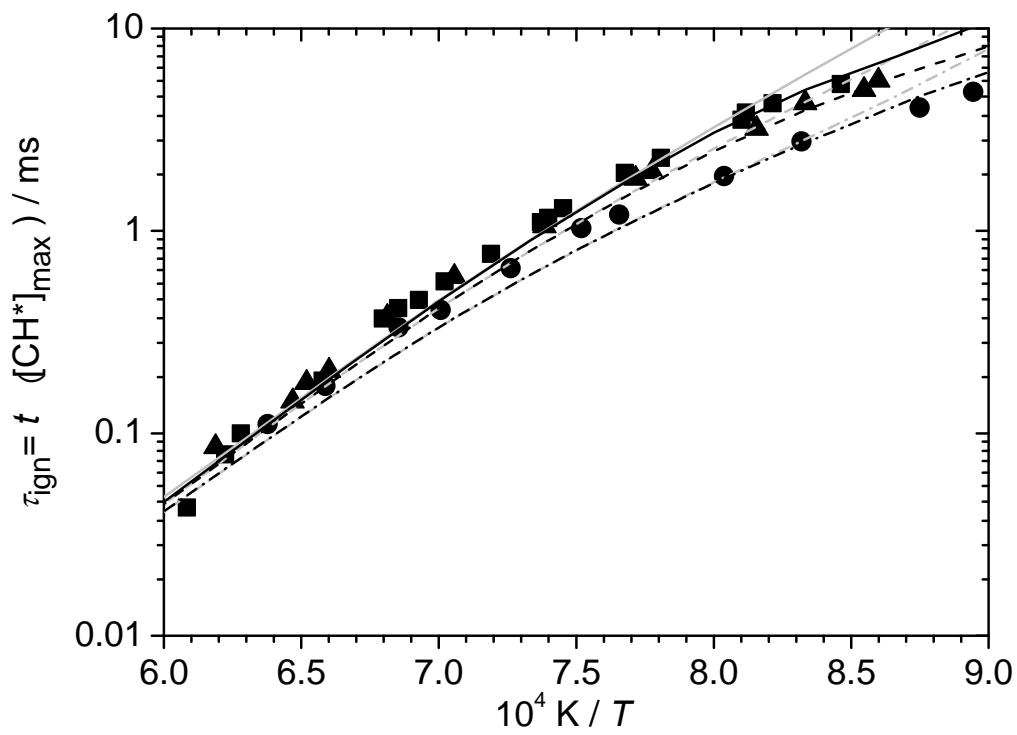


Figure 13

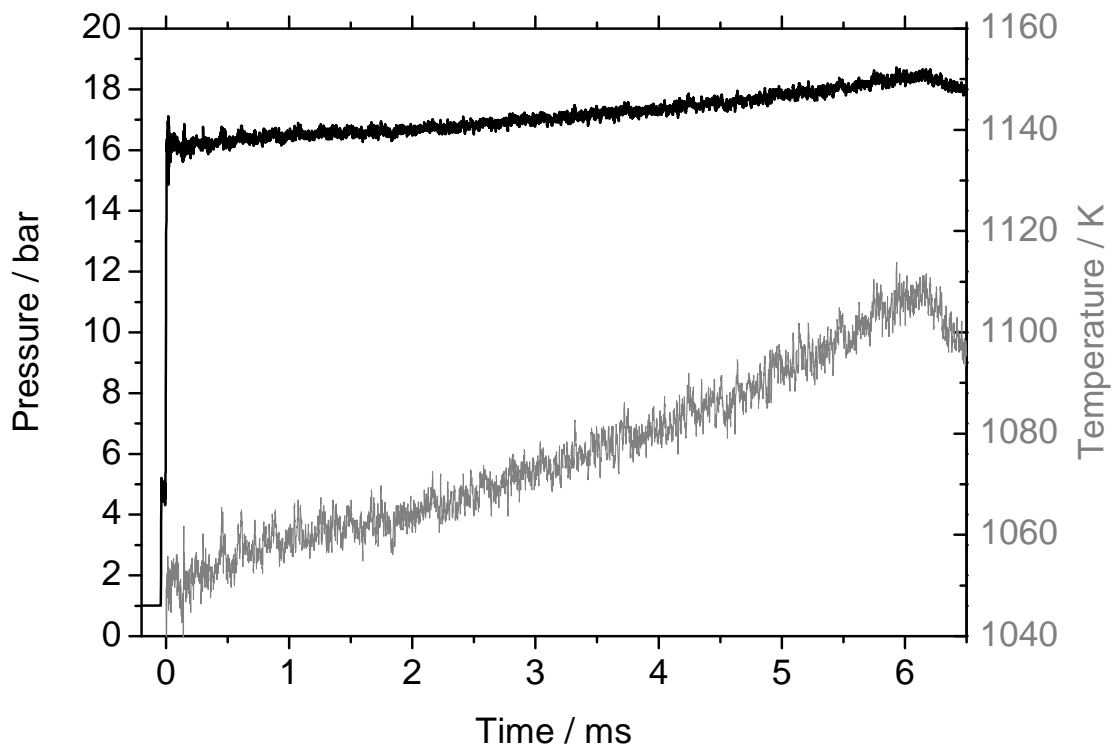


Figure 14

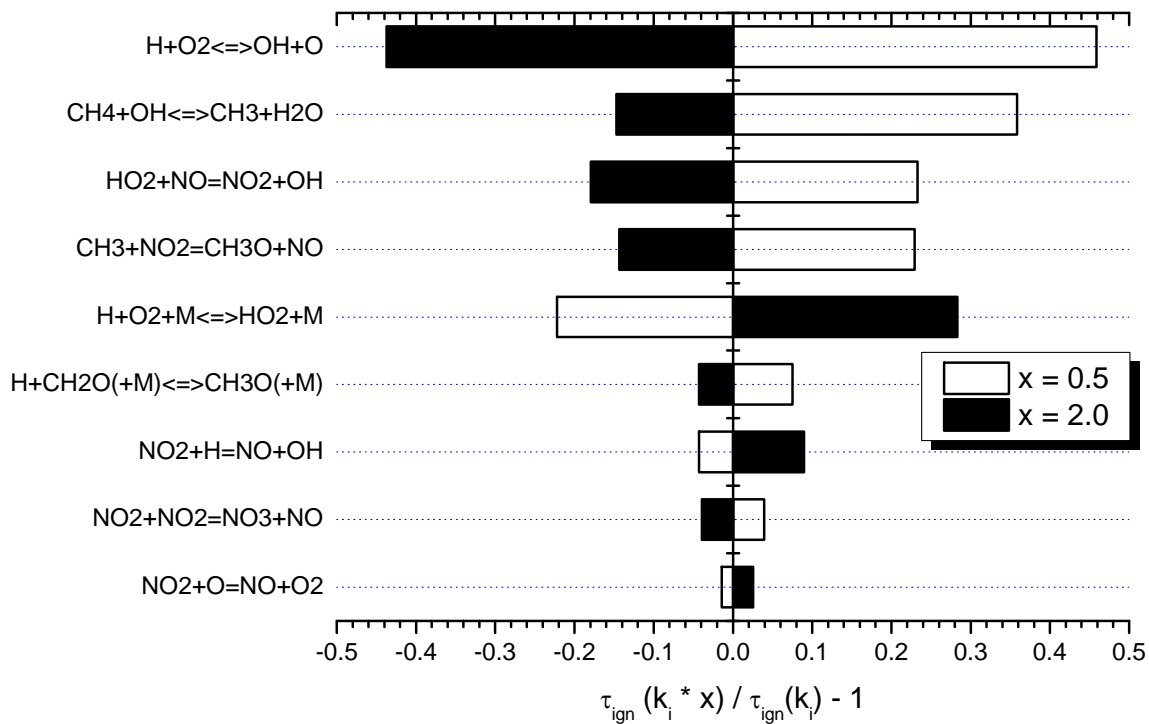


Figure 15

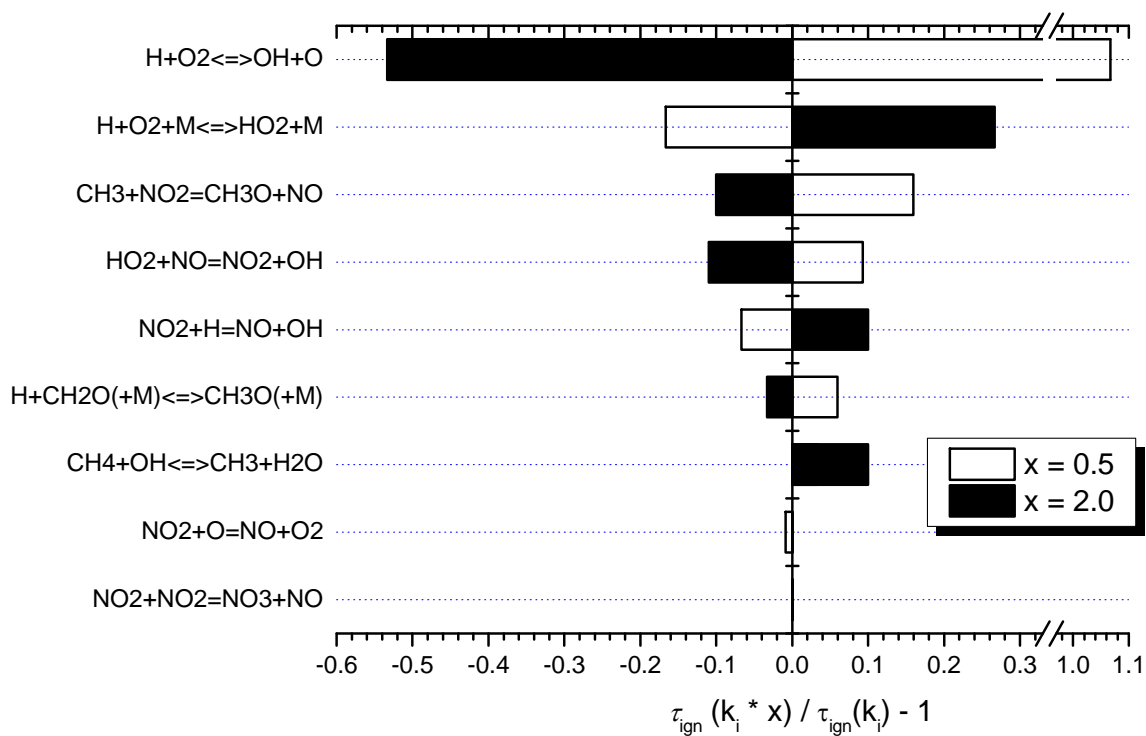


Figure 16

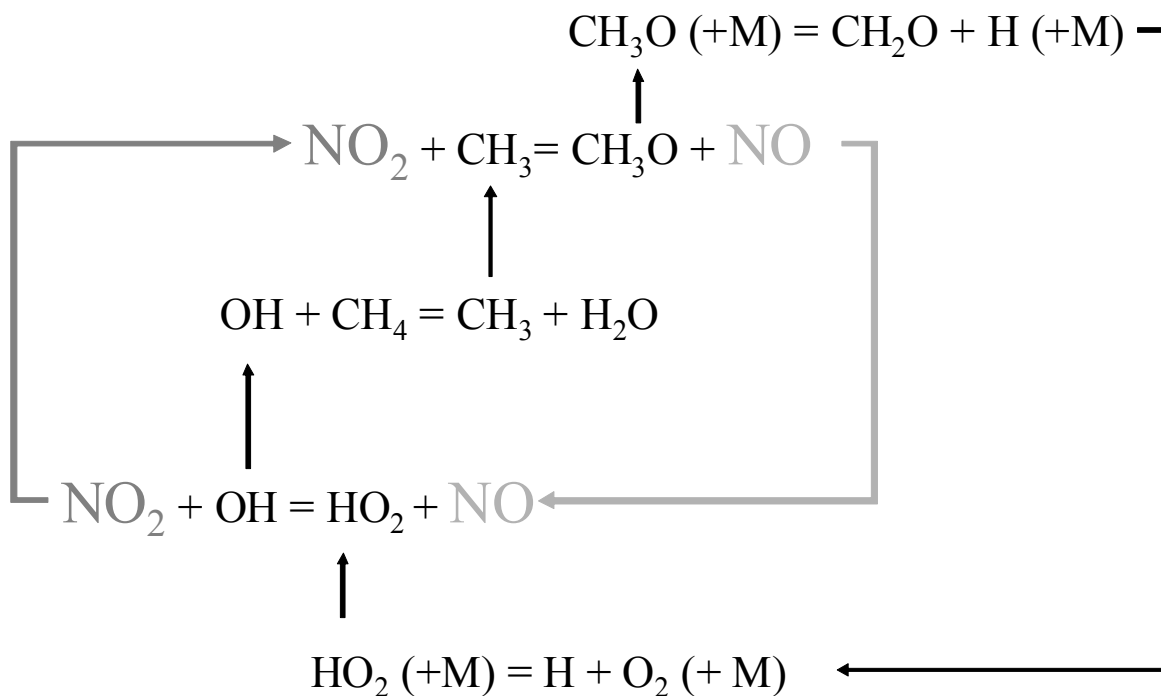


Figure 17

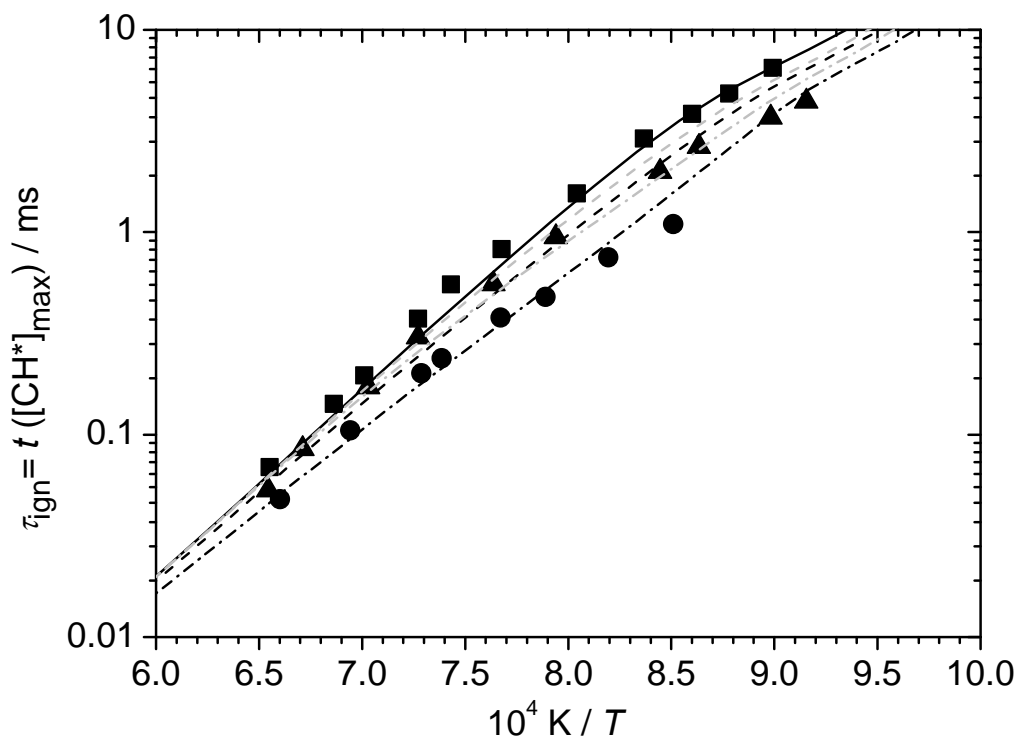


Figure 18

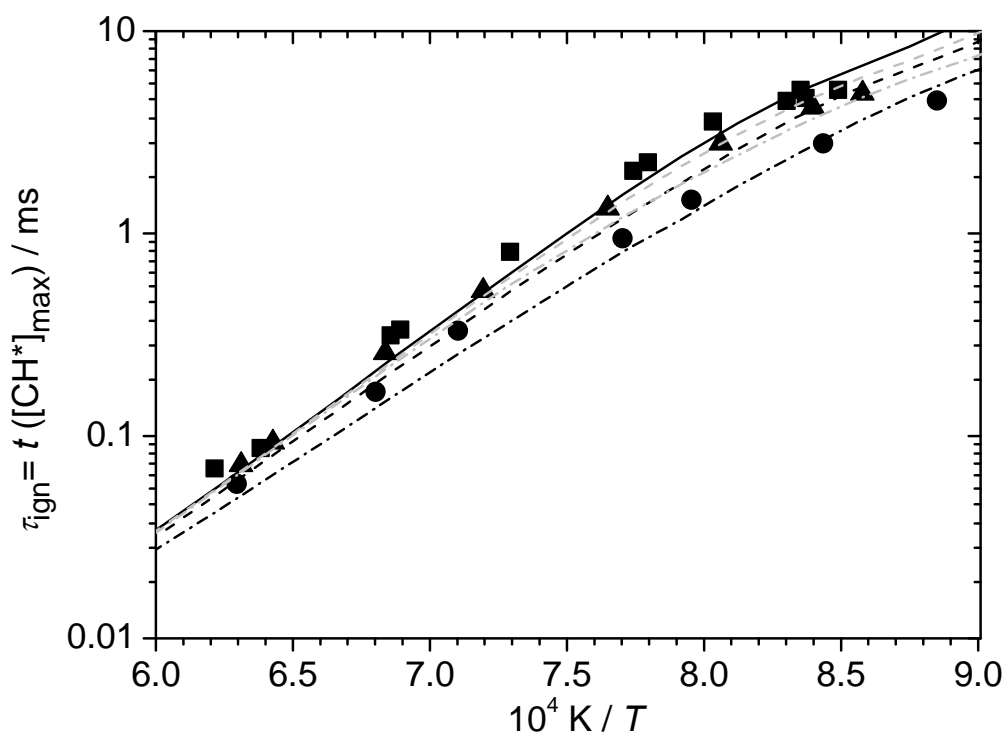


Figure 19

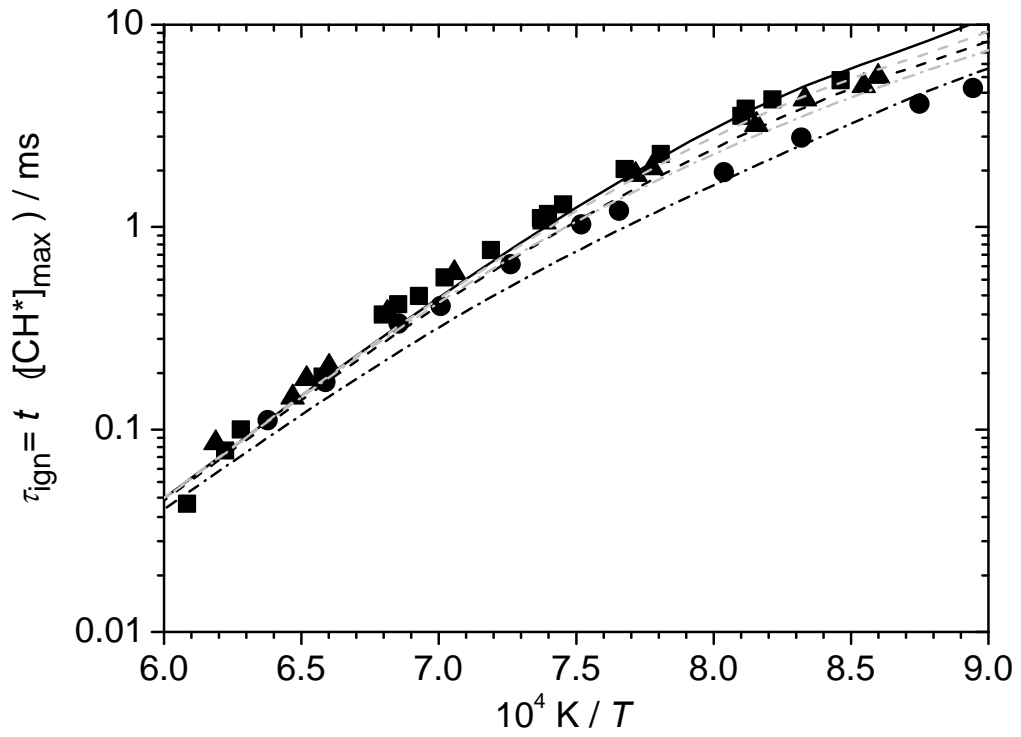
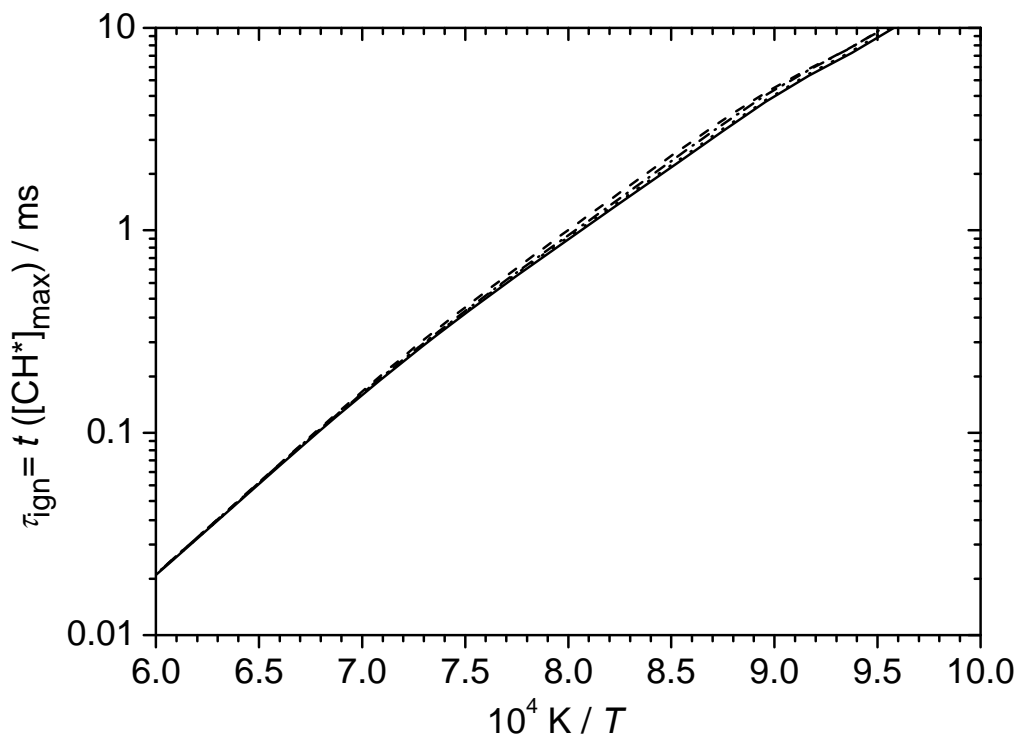


Figure 20



List of supplemental material:
 Table S1: Composition of the mixtures
 Table S2: Experimental results

Table S1: Composition of the mixtures.

Mixture	ϕ	dilution	CH ₄	C ₂ H ₆	NO ₂	O ₂	Ar
Reference gas	0.25	1:2	0.011074	0.000963	-	0.102282	0.885681
Reference gas / 50 ppm NO ₂	0.25	1:2	0.011160	0.000960	0.000050	0.103394	0.884437
Reference gas / 251 ppm NO ₂	0.25	1:2	0.011188	0.000950	0.000251	0.102974	0.884637
Reference gas	0.25	1:5	0.004339	0.000361	-	0.040641	0.954659
Reference gas / 20 ppm NO ₂	0.25	1:5	0.004388	0.000377	0.000020	0.040651	0.954564
Reference gas / 101 ppm NO ₂	0.25	1:5	0.004509	0.000383	0.000101	0.041505	0.953502
Mixture	ϕ	dilution	CH ₄	C ₂ H ₆	NO ₂	O ₂	Ar
Reference gas	0.5	1:5	0.008589	0.000734		0.039964	0.950713
Reference gas / 20 ppm NO ₂	0.5	1:5	0.008789	0.000757	0.000020	0.040164	0.950270
Reference gas / 100 ppm NO ₂	0.5	1:5	0.008637	0.000751	0.000100	0.039832	0.950680
100% reference gas	1.0	1:5	0.016643	0.001414	-	0.039226	0.942717
Reference gas / 103 ppm NO ₂	1.0	1:5	0.016587	0.001439	0.000103	0.038256	0.943616

Table S2: Experimental results.

Reference gas, $\Phi = 0.25$, dilution 1:2		
T / K	p / bar	τ / μ s
1112	16.78	6466
1139	16.76	4842
1163	16.66	3831
1195	16.87	2905
1244	16.39	1552
1303	16.59	823
1346	16.77	551
1375	15.60	374
1426	16.32	196
1457	15.92	142
Reference gas, $\Phi = 0.25$, dilution 1:2, 50 ppm NO ₂		
T / K	p / bar	τ / μ s
1092	16.53	4422

1113	18.00	3678
1158	17.44	2643
1184	16.47	1991
1259	16.73	947
1309	15.97	554
1375	16.52	303
1422	16.32	171
1490	15.62	85
Reference gas, $\Phi = 0.25$, dilution 1:2, 251 ppm NO ₂		
<i>T / K</i>	<i>p / bar</i>	<i>$\tau / \mu\text{s}$</i>
1175	17.29	1095
1220	16.50	752
1267	16.82	479
1303	16.76	378
1354	17.02	238
1372	16.46	201
1440	15.61	105
1515	15.68	48
Reference gas, $\Phi = 0.25$, dilution 1:5		
<i>T / K</i>	<i>p / bar</i>	<i>$\tau / \mu\text{s}$</i>
1178	16.38	5110
1195	16.27	4659
1197	15.91	5119
1204	16.96	4516
1245	16.55	3565
1283	16.38	2242

1292	15.90	2034
1371	16.48	811
1451	17.07	335
1459	17.38	314
1567	16.02	87
1609	15.74	69
Reference gas, $\phi = 0.25$, dilution 1:5, 20 ppm NO ₂		
<i>T</i> / K	<i>p</i> / bar	τ / μ s
1166	16.66	4918
1191	16.51	4204
1241	16.31	2789
1307	16.42	1330
1390	16.25	522
1463	15.64	257
1556	16.35	93
1585	15.41	72
Reference gas, $\phi = 0.25$, dilution 1:5, 101 ppm NO ₂		
<i>T</i> / K	<i>p</i> / bar	τ / μ s
1130	16.48	4532
1185	16.46	2785
1257	16.61	1468
1298	15.92	945
1408	16.35	331
1470	15.86	165
1589	15.60	58

Reference gas, $\Phi = 0.5$, dilution 1:5		
T / K	p / bar	$\tau / \mu\text{s}$
1182	16.44	5310
1217	15.94	4263
1232	15.73	3833
1234	15.74	3545
1281	15.78	2296
1303	16.37	1929
1342	15.63	1293
1352	16.56	1157
1356	15.70	1105
1391	15.47	769
1424	14.45	562
1443	14.42	455
1459	15.81	415
1471	16.06	369
1520	15.06	182
1592	15.95	100
1607	15.55	78.5
1643	17.27	43
Reference gas, $\Phi = 0.5$, dilution 1:5, 20 ppm NO ₂		
T / K	p / bar	$\tau / \mu\text{s}$
1163	15.78	5538
1170	16.57	4973
1200	16.38	4277
1226	16.56	3196
1286	16.87	1956

1296	16.30	1814
1354	16.02	1056
1417	16.02	594
1468	15.83	377
1515	15.24	204
1534	16.07	178
1546	15.71	144
1616	16.30	86
Reference gas, $\Phi = 0.5$, dilution 1:5, 100 ppm NO ₂		
<i>T</i> / K	<i>p</i> / bar	τ / μ s
1118	16.23	4852
1143	16.02	4065
1202	16.59	2757
1244	16.57	1862
1306	16.65	1203
1330	15.51	1029
1377	16.33	654
1427	16.35	407
1459	15.65	334
1518	16.10	171
1568	15.37	111
Reference gas, $\Phi = 1.0$, dilution 1:5		
<i>T</i> / K	<i>p</i> / bar	τ / μ s
1203	16.13	5436
1258	15.78	3571
1321	15.42	1987

1379	15.71	1286
1421	15.43	854
1466	15.29	537
1517	15.14	345
1560	15.26	200
Reference gas, $\Phi = 1.0$, dilution 1:5, 103 ppm NO ₂		
T / K	p / bar	$\tau / \mu\text{s}$
1133	16.07	5555
1197	16.18	3932
1214	16.33	3575
1214	15.66	3790
1264	15.91	2722
1295	15.77	2154
1333	15.78	1626
1409	15.23	847
1484	15.55	428
1529	15.48	298
1591	15.32	170
1626	14.25	106